

# Timescales of Oxygenation Following the Evolution of Oxygenic Photosynthesis

Lewis M. Ward<sup>1</sup>  · Joseph L. Kirschvink<sup>1</sup> · Woodward W. Fischer<sup>1</sup>

Received: 8 June 2015 / Accepted: 6 August 2015 /

Published online: 19 August 2015

© Springer Science+Business Media Dordrecht 2015

**Abstract** Among the most important bioenergetic innovations in the history of life was the invention of oxygenic photosynthesis—autotrophic growth by splitting water with sunlight—by Cyanobacteria. It is widely accepted that the invention of oxygenic photosynthesis ultimately resulted in the rise of oxygen by *ca.* 2.35 Gya, but it is debated whether this occurred more or less immediately as a proximal result of the evolution of oxygenic Cyanobacteria or whether they originated several hundred million to more than one billion years earlier in Earth history. The latter hypothesis involves a prolonged period during which oxygen production rates were insufficient to oxidize the atmosphere, potentially due to redox buffering by reduced species such as higher concentrations of ferrous iron in seawater. To examine the characteristic timescales for environmental oxygenation following the evolution of oxygenic photosynthesis, we applied a simple mathematical approach that captures many of the salient features of the major biogeochemical fluxes and reservoirs present in Archean and early Paleoproterozoic surface environments. Calculations illustrate that oxygenation would have overwhelmed redox buffers within ~100 kyr following the emergence of oxygenic photosynthesis, a geologically short amount of time unless rates of primary production were far lower than commonly expected. Fundamentally, this result arises because of the multiscale nature of the carbon and oxygen cycles: rates of gross primary production are orders of magnitude too fast for oxygen to be masked by Earth's geological buffers, and can only be effectively matched by respiration at non-negligible O<sub>2</sub> concentrations. These results suggest that oxygenic photosynthesis arose shortly before the rise of oxygen, not hundreds of millions of years before it.

**Keywords** Great oxidation event · Phototrophy · Methane · Aerobic respiration · Biogeochemistry

---

✉ Lewis M. Ward  
LWARD@caltech.edu

<sup>1</sup> Division of Geological and Planetary Sciences, California Institute of Technology, 1200 E. California Blvd, Pasadena, CA 91125, USA

## Introduction

Sometime between 2.4 and 2.35 billion years ago (Gya) the Earth experienced one of its largest and most significant changes, when free molecular oxygen first accumulated in the atmosphere (Bekker et al. 2004; Papineau et al. 2007; Guo et al. 2009; Hoffman 2013; Johnson et al. 2013a, 2014; Rasmussen et al. 2013a). This event has long been recognized from a wide range of geological and geochemical proxies (Fig. 1), and is thought to be caused by the metabolic products of oxygenic Cyanobacteria (e.g., Falkowski 2011; Shih 2015). However, there is a long history of interpretations and hypotheses regarding the greater antiquity of Cyanobacteria deep into Archean time that have proven controversial. Interpretations in support of Cyanobacteria in Paleoproterozoic time once included putative cyanobacterial microfossils from the Archean Apex Chert (Schopf 1993), which remain uncertain as body fossils regardless of phylogenetic affinity (Brasier et al. 2002). Even if these structures are proven to be microfossils, convergence of morphology makes the interpretation of these and other filamentous microfossils as Cyanobacteria equivocal (Knoll and Golubic 1992; Shih et al. 2013). Similarly, stromatolites—accretionary sedimentary growth structures often interpreted to be formed by the interaction of microbial mats and sediment—have been interpreted as

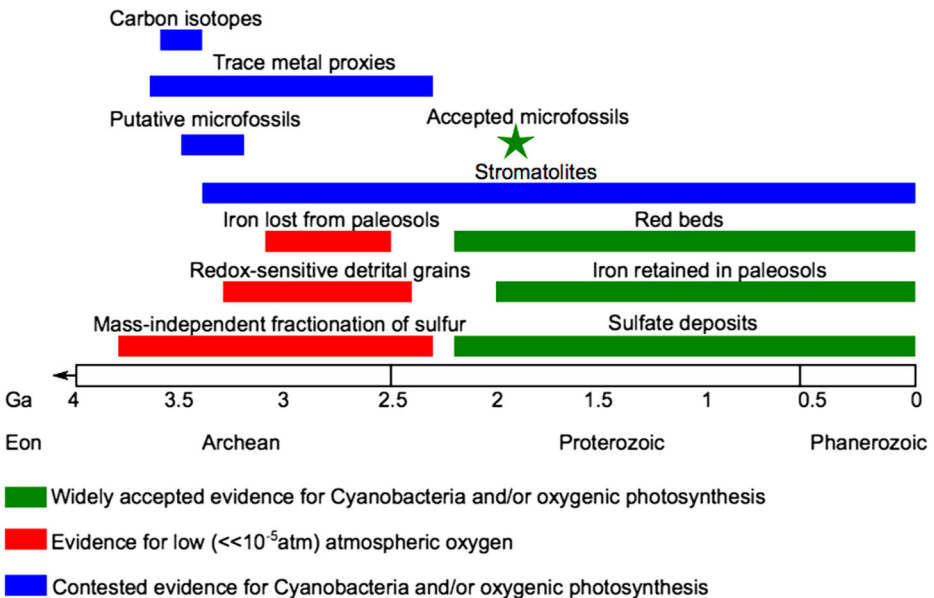


**Fig. 1** Earth history timeline with key geological and geochemical records of oxygen and Cyanobacteria noted. The rise of oxygen has been dated to *ca.* 2.35 Gya based on the disappearance of mass-independent fractionation of sulfur (Rasmussen et al. 2013a). This is consistent with other proxies for a transition in the oxygenation state of the atmosphere at this time such as the disappearance of redox-sensitive detrital grains (Johnson et al. 2014), the behavior of iron in paleosols and red beds (Holland 1984), and the appearance of evaporative sulfate mineral deposits (Chandler 1988). The oldest widely accepted cyanobacterial microfossils are those of *Eoentophysalis sp.* in rocks *ca.* 1.9 Ga. Also noted are several controversial pieces of evidence for Cyanobacteria and/or oxygen in older rocks. These include putative microfossils at *ca.* 3.5 Ga (Schopf 1993); stromatolites, with a record beginning *ca.* 3.4 Ga (Hofmann et al. 1999; Allwood et al. 2006); carbon isotope values in graphite and kerogen (Schidlowski et al. 1979; Rosing 1999); and various trace metal proxies interpreted as recording local or transient oxygen enrichments between *ca.* 3.7 and 2.5 Ga (Rosing and Frei 2004; Anbar et al. 2007; Planavsky et al. 2014; Crowe et al. 2013)

cyanobacterial products in deep time. The stromatolite record dates back more than 3.4 Ga (Hofmann et al. 1999; Allwood et al. 2006), with many stromatolites interpreted as being formed by Cyanobacteria (e.g., Buick 1992). However, it has been proposed that ancient stromatolites need not have been formed by Cyanobacteria (Brock 1978; Bosak et al. 2007), and hypothesized that not all stromatolites are formed biogenically (Grotzinger and Knoll 1999), making the relationship between them and Cyanobacteria uncertain. Schidlowski and colleagues (1975, 1979) argued on the basis of carbonate carbon isotope values that oxygenic photosynthesis had been in place since at least 3.7 Gya, with Rosing and Frei (2004) reaching the same conclusion from observations of  $^{13}\text{C}$ -depleted graphite and relatively high lead concentrations in graphite-bearing quartz±garnet schists of similar age; however, none of these features may be diagnostic of oxygenic photosynthesis (Kopp et al. 2005). The discovery of 2-methylhopane biomarkers in Archean rocks has also been used to argue for Cyanobacteria predating the rise of oxygen (Brocks et al. 1999), although from subsequent studies it has been recognized that these molecules are not unique to Cyanobacteria (Rashby et al. 2007; Welander et al. 2010), likely evolved in other phyla (Ricci et al. 2015), and may not even be native to the rocks (French et al. 2015). Most recently, a range of data from trace metal proxies have been interpreted as “whiffs” of oxygen in Archean surface environments, more specifically spatially or temporally local pulses of cyanobacterial  $\text{O}_2$  that left a record in trace metal oxygen proxies but failed to fully or irreversibly oxidize the atmosphere (Anbar and Knoll 2002; Kaufman et al. 2007). Recent trace metal data from strata nearly three billion years old have been interpreted to show evidence of oxygenic photosynthesis (Planavsky et al. 2014; Crowe et al. 2013). The interpretation of these trace metal signatures of  $\text{O}_2$  remains controversial in part because their geochemical cycles are not well understood both in modern environments and in diagenetically stabilized and post-depositionally altered lithologies typical of Precambrian successions (Helz et al. 2011; Nägler et al. 2011; Morford et al. 2012); these whiff signatures also appear to conflict with independent geochemical  $\text{O}_2$  proxies such as redox-sensitive detrital grains and mass independent fractionation of sulfur isotopes (e.g., Johnson et al. 2014). Furthermore, the long stretch of geological time over which whiffs are thought to have occurred is at odds with expectations for the productivity of oxygenic photosynthesis, and so limits to the spread of oxygen are invoked (e.g., Lyons et al. 2014). These arguments often rely on redox buffers, geologically-sourced reduced compounds in the atmosphere and/or oceans (like  $\text{Fe}^{2+}$  or  $\text{CH}_4$ ), which reacted with molecular oxygen to prevent its environmental accumulation (Schidlowski 1983; Gaillard et al. 2011; Kump and Barley 2007). The depletion of these redox buffers over geological time due either to changes in source fluxes or reaction with oxygen is thought to eventually allow oxygen to rise (e.g., Holland 2009). The “rusting” of the fluid Earth has long been considered as a mechanism for the deposition of banded iron formations (Cloud 1973; Walker et al. 1983), though these deposits are now recognized to have much more complex origins and are comprised of dominantly ferrous mineral products from an iron cycle that need not have involved molecular oxygen (Fischer and Knoll 2009; Rasmussen et al. 2013b). Ultimately, however, it remains unclear how well geological processes and redox buffers might counter the large fluxes and rapid responses anticipated of biological productivity.

Massive numbers characterize the modern oxygen cycle, including fluxes that appear capable of responses to perturbations on extremely short timescales. The atmosphere currently contains nearly 21 % dioxygen by volume ( $\sim 3.8 \times 10^{19}$  moles  $\text{O}_2$ ), and this concentration is thought to have been largely stable at least since the beginning of the Cenozoic Era (Glasspool and Scott 2010). Global annual net primary productivity (NPP) is estimated from

measurements of carbon fluxes to be on the order of 105 Pg C/year, an amount equivalent to  $\sim 8.75 \times 10^{16}$  moles of  $O_2$  per year (Field et al. 1998), giving a residence time of  $O_2$  in the atmosphere of only about 4300 years. Such a short residence time of atmospheric  $O_2$  is further supported by O isotope ratio data on  $O_2$  from gas trapped within ice cores, which shows large and rapid variation over geologically short (<1 kyr) timescales, implying a residence time for  $O_2$  in the atmosphere perhaps as short as a couple of hundred years (Severinghaus et al. 2009). Thus any accurate first order description of the oxygen cycle should capture these rapid dynamics. Indeed it is remarkable that atmospheric oxygen appears to remain stable over a range of timescales (e.g., Suwa and Bender 2008; Berner 1989) despite rapid turnover and variability in global primary productivity over glacial/interglacial timescales (Bender et al. 1994; Paytan et al. 1996) to Phanerozoic timescales (Robinson 1990). Tight feedbacks must be in place to maintain oxygen concentrations.

The largest sink in the oxygen cycle is that of aerobic respiration. While gross primary productivity (GPP, the rate at which organic carbon is fixed by organisms) is very large, about half of all fixed carbon is respired by plants and algae themselves (Bender et al. 1999). The remaining fixed carbon is referred to as net primary productivity (NPP), and the vast majority of this is remineralized by heterotrophs. Only a small fraction is ultimately buried and allows the accumulation of  $O_2$  in the atmosphere, on the order of 0.32 % of NPP (Berner 1989). This tight coupling of primary production and aerobic respiration has maintained a stably oxygenated atmosphere over Phanerozoic time (Glasspool and Scott 2010), but this balance may not have applied soon after oxygenic photosynthesis evolved, as efficient mechanisms for aerobic respiration may not have evolved until after the evolution of oxygenic photosynthesis (Gribaldo et al. 2009). Furthermore, aerobic respiration typically requires a threshold concentration of  $O_2$  in the environment to be efficient, with most organisms transitioning to anaerobic metabolism at oxygen concentrations lower than  $\sim 3 \mu M$ , near what is known as the Pasteur Point (Canfield 2005). Slow growth of a strain of *Escherichia coli* was observed to occur at lower, nanomolar oxygen concentrations (Stolper et al. 2010), though the ecological and environmental relevance of these results has been questioned (Ducluzeau et al. 2014). The evolutionary timing and oxygen requirements of aerobic respiration remain important open questions, but it is reasonable to infer that early respiration was slow due to oxygen concentrations far below the concentrations at which respiratory enzymes optimally function (e.g., Guo et al. 2009). The largest control on preservation of organic carbon in the sediments is oxygen exposure time (Hartnett et al. 1998). As oxygen exposure time would be much lower before and during the rise of oxygen, organic carbon burial efficiency would almost certainly be higher than today. This is supported by measurements of organic carbon burial rates in Lake Matano, an interesting Archean analog site, where burial rates are on the order of 22 % of NPP (Crowe et al. 2011). Lake Matano is a permanently stratified lake in Indonesia and is considered one of the best extant Archean ocean analog systems due to its photic zone anoxia, high dissolved iron content, and low sulfur content (Crowe et al. 2008, 2011; Jones et al. 2011). The absence of aerobic respiration before the rise of oxygen likely required alternative remineralization processes to play larger roles in the carbon cycle, most likely dominated by methanogenesis (Hayes 1994). This has been observed in Lake Matano, where methanogenesis appears to be responsible for  $\sim 50$  % of organic carbon remineralization (Crowe et al. 2011).

Until oxygen concentrations were reached that made aerobic respiration an efficient  $O_2$  sink,  $O_2$  sourced from oxygenic phototrophs would largely titrate reduced compounds such as methane and ferrous iron in seawater and the atmosphere—redox buffers that might prevent

accumulation of oxygen in the atmosphere depending on their relative abundances and reaction kinetics (Lyons et al. 2014). It is critical to note here that many of these redox buffers are ultimately replenished on geological (i.e., chemical weathering) timescales—these are slow relative to phototrophic oxygen fluxes. This mismatch of timescales suggests the hypothesis that, because redox buffers would have been replenished sufficiently slowly, O<sub>2</sub> would have accumulated rapidly from the perspective of geological time. To test this idea and quantitatively determine whether these limitations would be sufficient to slow the oxygenation of the atmosphere over the long term, we present a geochemical box model of the Archean Earth that includes a realistic assessment of the oxygen sinks possibly present in the environment. Rather than hundreds of millions of years, we find that oxygenation should have happened in tens of thousands to perhaps a hundred thousand years after oxygenic photosynthesis evolved in Cyanobacteria.

## Basic Accounting

An initial, simple estimate of the time necessary to oxygenate the atmosphere can be determined simply by summing the pools of reduced “redox buffer” compounds in the atmosphere and ocean and dividing these by the gross O<sub>2</sub> flux. Using estimates of reduced compound concentrations and rates of productivity and carbon burial detailed below, this results in the consumption of all stored reducing power on Earth’s surface within a few hundred years. While this serves as no more than a rough approximation, it highlights that despite the overall reduced state of the Archean Earth, absolute abundances of redox buffer compounds are small compared to the anticipated fluxes of oxygen produced through oxygenic photosynthesis. A more sophisticated oxygenation model, accounting for geological and biological fluxes of reductants into the Earth system, is detailed below.

## Model Summary

We follow the estimates detailed below for Archean starting concentrations and fluxes of each oxygen sink. However, we make a number of simplifying assumptions, including: (1) the oceans are of the same volume as the modern ( $\sim 1.3 \times 10^{21}$  liters), (2) the atmosphere was made up of the same number of gas molecules as today ( $\sim 1.8 \times 10^{20}$  moles), and (3) primary productivity driven by anoxygenic photosynthesis is minor relative to oxygenic photosynthesis (e.g., Kharecha et al. 2005). Furthermore, (4) we note that the net reactions that describe anoxygenic photosynthesis are equivalent to oxygenic photosynthesis when O<sub>2</sub> equivalents are measured (e.g., iron oxides are produced equivalently by direct photosynthetic oxidation or via oxidation by O<sub>2</sub> produced from oxygenic photosynthesis). This allows us to consider primary productivity as a single flux. Additionally, (5) we ignore sulfide fluxes because any such input into the fluid Earth will be removed as pyrite as it reacts with ferrous iron in the predominantly ferruginous oceans. This follows logic from Walker and Brimblecombe (1995), whereby larger geochemical iron sources will lead to removal of sulfur unless the iron is first immobilized by oxidation. As this will also serve as a sink for reduced iron, ignoring sulfide can be considered a conservative estimate. Next, (6) the ocean is assumed to be well-mixed with regards to chemical compounds and microbial populations. While ocean and atmospheric circulation are important factors in controlling the distribution of microbes and geochemical compounds,

these processes are relatively rapid, on the order of  $\sim 1$  kyr—a timescale much finer than the typical resolution of the sedimentary record (Sadler 1981). While the oceans likely cannot stagnate completely, they can be dynamically stratified as a result of changes in circulation patterns (e.g., Hotinski et al. 2000, 2001), but even if mixing were substantially slower this would only serve to isolate reduced compounds to the deep ocean and would allow the surface oceans and the atmosphere to oxidize even faster. Similarly, oxidation rates of all species by  $O_2$  is considered to be geologically instantaneous, so kinetic reaction rates are ignored. However, rates are included in the particular cases of hydrogen escape and methane photolysis, as these are driven by processes other than the production of  $O_2$ .

**Reduced Pools** A number of pools of reduced compounds are expected to be present in the ocean and atmosphere before the rise of oxygen, and are summarized in Fig. 2. Major atmospheric reduced species include hydrogen and methane. Estimates of atmospheric mixing ratios of 0.001 (i.e., 1000 ppmv, or 1 permil) for these species were derived from Pavlov et al. (2000) [later estimates by Haqq-Misra et al. (2011) revised estimates for Archean  $H_2$  mixing ratio down to 0.0003, but we use here the earlier, higher value as a conservative estimate]. These represent upper bounds for the concentrations of each of these species in order to satisfy the Faint Young Sun paradox (Pavlov et al. 2000). If the Faint Young Sun is instead counteracted by, for instance, high concentrations of  $CO_2$  as has been elsewhere proposed (Owan et al. 1979), these concentrations may be substantially lower and would lower existing reduced pools and accelerate atmospheric oxidation; we therefore utilize these upper concentration ranges as a conservative estimate.

Major aquatic reduced pools are dissolved  $Fe^{2+}$ ,  $Mn^{2+}$ , and ammonia. Estimates were derived from Holland (1984) and Canfield et al. (2010), and range up to 120 micromolar for iron and manganese, and 80 micromolar for ammonia. Metal concentration estimates come from the solubility of their respective carbonate species, while ammonium concentrations were

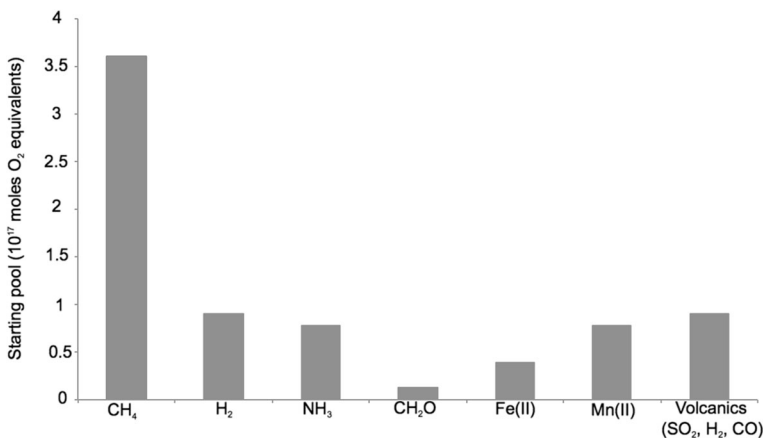


**Fig. 2** Estimated starting pools of reduced compounds given as moles of  $O_2$  equivalents (e.g., 1 mole of  $Fe^{2+}$  is 0.25 moles of  $O_2$  equivalents, as it requires 0.25 moles of  $O_2$  to oxidize 1 mole of  $Fe^{2+}$  to  $Fe^{3+}$ ).  $H_2$  and  $CH_4$  are estimated at 0.001 atm (Pavlov et al. 2000).  $Fe^{2+}$  and  $Mn^{2+}$  are estimated at up to 120 micromolar (Holland 1984). Ammonia is estimated at 80 micromolar (Canfield et al. 2010). While dissolved iron in the oceans is frequently cited as buffering the Archean Earth against oxidation, the relatively low concentrations of iron and its oxidation stoichiometry make it relatively insignificant compared to other compounds like methane

based on an assumption of nutrient co-limitation with iron by anoxygenic phototrophs prior to the advent of oxygenic photosynthesis. Large ranges of possible concentrations were proposed; the highest estimates were used here.

**Reduced Fluxes** Fluxes of reduced compounds to the atmosphere and oceans from processes such as hydrothermal cycling and volcanic outgassing are summarized in Fig. 3. Fluxes of reduced compounds from volcanoes were estimated based on Holland (2002) to be a combined  $1.4 \times 10^{12}$  moles of  $\text{SO}_2$ ,  $\text{CO}$ , and  $\text{H}_2$  with identical oxidation stoichiometries. If  $\text{H}_2$  is a significant volcanic gas, this could increase overall rates of hydrogen escape, driving an  $\text{O}_2$ -independent sink of reducing power, increasing the rate of atmospheric oxidation. Pooling all volcanic gases therefore provides a conservative estimate.

Production of oceanic crust and associated reduced iron was derived from Lécuyer and Ricard (1999). Based on Williams et al. (2012), it is assumed that mantle redox—and therefore the  $\text{Fe}^{2+}/\text{Fe}^{3+}$  ratio of new crustal material—has been constant since accretion.

Hydrothermal fluxes were derived from Elderfield and Schultz (1996) for modern values as a reference, and Archean fluxes are naively assumed to be ten times modern based on Des Marais (2000), although it is possible that Archean hydrothermal fluxes were lower than modern (e.g., Korenaga 2006). While  $\text{Fe}^{2+}$  is here given as a major component of hydrothermal fluxes, this iron is sourced from weathering of newly formed crust. Because it is tricky to untangle this, this iron is therefore essentially double-counted in our model here to provide a conservative oxygenation timescale estimate.

Biogenic methane fluxes are largely unconstrained for Archean time, but solutions for the Faint Young Sun paradox using methane as a greenhouse gas assume comparable fluxes to the modern (e.g., Pavlov et al. 2001)—an estimate arrived at independently by Kharecha et al. (2005). This is equivalent to about 8 % of remineralized organic matter being converted to methane given the rates of primary productivity used in this model. Estimates for

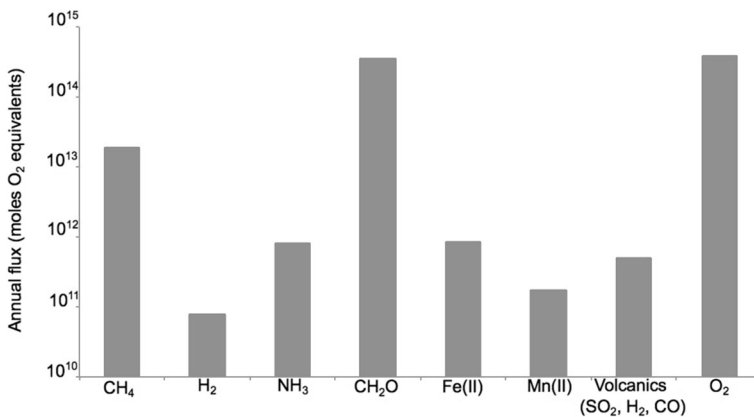


**Fig. 3** Fluxes of reduced compounds and  $\text{O}_2$  given as moles of  $\text{O}_2$  equivalents per year. Volcanic gases (Holland 2002),  $\text{Fe}^{2+}$  (Lécuyer 1999), hydrothermal fluxes of other compounds derived from modern fluxes collected by Elderfield and Schultz (1996) and using the high estimate of  $10\times$  modern hydrothermal fluxes from Des Marais (2000).  $\text{O}_2$ , organic carbon, and methane fluxes are variables in our model, and conservative estimates (Scenario A in Table 1) are given here. Primary production fluxes dwarf fluxes of reduced compounds, making them a dominant control on the model results

methanogenic rates can also be made by analogy to Lake Matano (Crowe et al. 2008). It has been demonstrated that in Lake Matano, 50 % or more of fixed organic carbon is remineralized via methanogenesis (Crowe et al. 2011). This is consistent with estimates from Hayes (1994), who hypothesized from carbon isotope mass balance that  $\text{CO}_2$  and  $\text{CH}_4$  were equally significant for Archean carbon cycling.

**Oxidizing Fluxes** Photolysis of methane, and hydrogen escape to space are modeled as first order reactions with time constants based on rates from Catling et al. (2001), resulting in a net loss of reducing power from the Earth system over time without consumption of  $\text{O}_2$ . Methane photolysis in the Archean atmosphere is expected to be limited by concentrations of hydroxyl radicals derived from  $\text{H}_2\text{O}$  photolysis, and so is expected to be  $\sim 1000$  times slower than modern methane breakdown in an oxygen-rich atmosphere (Pavlov et al. 2000). The flux of fixed carbon to methane is a significant variable in this model. As methane can be lost from the Earth system through an  $\text{O}_2$ -independent photolytic reaction, it acts as an absolute sink of electron equivalents, allowing oxygen to react with other reductants and eventually to build up. We have therefore used on a more conservative, low value for methanogenic flux.

While the nutrient status of Archean seawater is largely unknown, we take primary productivity as limited to 10 % of modern marine values due to phosphorous limitation as suggested by Bjerrum and Canfield (2002), resulting in  $3.8 \times 10^{14}$  moles carbon fixed per year. Phosphorous is generally assumed to be the limiting nutrient for marine productivity of geologic timescales (Tyrrell 1999) and nitrogen is assumed to be abundant in upwelling waters prior to the evolution of the aerobic nitrogen cycle (Canfield et al. 2010). Dissolved inorganic carbon is assumed to not be limiting for oxygenic photosynthesis, as DIC concentrations are thought to have been as high or higher than modern (Fischer et al. 2009). As a result, DIC would therefore have been greater than 2 mM in seawater, making these concentrations far in excess of other relevant redox-active dissolved species, and thus DIC concentrations do not place a strong limit on oxygenation in so far as coeval redox buffers like ferrous iron are concerned. Burial of organic carbon is assumed to be a similar fraction of primary productivity to the modern, based on Berner (1982), of about 0.32 %. Burial rates are considerably higher in modern anoxic basins—e.g., 2 % in the Black Sea (Arthur et al. 1994), and 22 % in Lake Matano (Crowe et al. 2011), and consequently this approach yields a highly conservative estimate because this parameter exerts strong control on the rate of oxygenation of the oceans and atmosphere.

**Model Calculations** The model topology consists of a simple box model with initial pools of reduced compounds (Fig. 2) that then through numerical simulations are both titrated by  $\text{O}_2$  and resupplied. The algorithm is iterated through time, at each step adding a flux of reduced compounds from geological processes as detailed below and in Fig. 3 and adding  $\text{O}_2$  according to the model parameter GPP. Reduced compounds are consumed by reaction with  $\text{O}_2$ , and additional oxidizing power is introduced through the escape of hydrogen and photolysis of methane. An example function for tracking a generic reduced compound X is:  $X(t) = X(t-1) + X_f * t$ , with  $X(0)$  equal to the starting pools in Fig. 2,  $X_f$  is the flux given in Fig. 3, and  $t$  is the time step over which the model is iterated. This form of equation is used for reduced compounds with the exceptions of methane and hydrogen, which are taken as functions following the modified form:  $X(t) = X(t-1) + X_f * t * e^{-c*t}$ , where  $c$  is a constant based on estimated lifetimes for these compounds in the Archean atmosphere (Catling et al. 2001).

Oxygen is then added to the system according to the chosen GPP value, and allowed to react with each compound. The model iterates through each compound as long as oxygen remains in the system, oxidizing them in a stoichiometric ratio as:  $X(t) = X(t) - \text{NetO}_2(t) / X_s$ , where  $X_s$  is the stoichiometry of the reaction and  $\text{NetO}_2$  is the number of moles of free  $\text{O}_2$ , beginning each step as  $\text{NetO}_2(t) = \text{NetO}_2(t-1) + \text{GPP} \cdot t$  but consumed through each step of reaction with reduced compounds:  $\text{NetO}_2(t) = \text{NetO}_2(t) - X(t) \cdot X_s$ . This proceeds at each step until either all  $\text{O}_2$  is consumed or all reduced compounds are oxidized, and the algorithm proceeds to the next step, allowing remaining  $\text{O}_2$  or reduced compounds to accumulate and persist to the next step. An example output of these calculations is given in Fig. 4, in terms of total  $\text{O}_2$  equivalents, equivalent to:  $\text{O}_2 \text{ Equivalents} = \sum X(t) \cdot X_s$ .

## Results

Under the parameters outlined above, the fluid Earth is oxidized (reduced pools consumed and oxygen begins to accumulate) in about 57 kyr (e.g., Fig. 4). This is rapid from the perspective of geological time. While there are uncertainties in these calculations, this suggests that redox buffers were not sufficient to delay oxygenation for hundreds of millions or billions of years. Varying parameters can lead to estimates of oxygenation a few times faster or slower (scenarios summarized in Table 1), but any realistic combination of values results in oxygenation within at most a few hundreds of thousands of years. Oxygen is then able to accumulate sufficiently to concentrations sufficient to largely eliminate mass independent fraction of atmospheric sulfur-bearing species (e.g., Pavlov and Kasting 2002) within a hundred or so years.

Despite substantial effort modeling the relationships between the core biogeochemical cycles and atmospheric oxygen, little prior work has explicitly addressed the timescales for oxygenation following the evolution of oxygenic photosynthesis. Previous studies that constructed mathematical models of the oxygen cycle typically employed flux estimates that were considered geologically relevant for the problem at hand (e.g., Berner 2006). While this approach is appropriate for the common geological timescales of integration, it smooths over

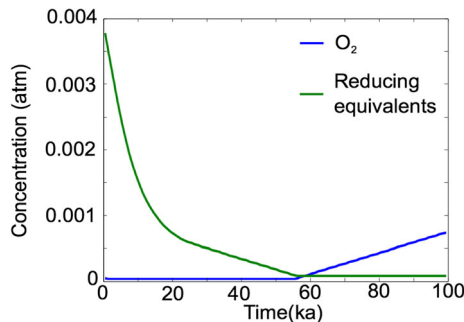


**Fig. 4** Example calculation, plotting total  $\text{O}_2$  equivalents and atmospheric  $\text{O}_2$  through time. Data plotted is for Scenario 1 (summarized in Table 1), a conservative estimate of oxygenation time based on the best estimates for Archean NPP (10 % of modern marine values based on phosphorous limitation, per Bjerrum and Canfield 2002), Archean methanogenic rates (0.1 of NPP, per Kharecha et al. 2005), and modern burial rates (0.32 % of NPP, per Berner 1982). Once oxygenic photosynthesis is initiated, net  $\text{O}_2$  (that remaining after reaction with annual reductant fluxes) begins to consume starting pools of reduced compounds. These are depleted after ~57 kyr, at which time free  $\text{O}_2$  accumulates

**Table 1** Model solutions for a range of potential conditions

Scenario:	GPP (moles C, O <sub>2</sub> /year):	Burial fraction:	Methanogenic fraction:	Oxygenation timescale (ka):	Notes
A	$3.8 \times 10^{14}$	0.0032	0.1	57	Conservative estimate based on predicted Archean productivity and modern carbon cycle remineralization rates, scenario output shown in Fig. 4.
B	$3.8 \times 10^{14}$	0.22	0.5	7	Reasonable Archean estimates based on Lake Matano as an analog
C	$3.8 \times 10^{14}$	0.22	0	8	Scenario B with no methanogenesis
D	$0.19 \times 10^{14}$	0.22	0.5	65	Scenario B with low productivity
E	$3.8 \times 10^{14}$	0.25	0	7	Metabolically-limited (nomethanogenesis, inefficient remineralization)

many multiscale processes that have foundationally faster dynamics. For example, it is widely appreciated that burial and weathering (plus volcanic) fluxes are in balance on million year timescales for an atmosphere of ~20 % O<sub>2</sub> by volume. (e.g., Lasaga and Ohmoto 2002). However embedded within this, photosynthesis and respiration meet to balance each other on nearly annual timescales. Integrating the oxygen cycle at million year time steps implicitly removes these dynamics. It was our goal with this work here to capture some of this. It is important to note, however, that our results still conform to a number of prior findings regarding the oxygen cycle. Goldblatt and colleagues (2006) showed that the balance between photosynthetic oxygen production and geologic flux of reduced compounds is fundamental to determining steady state oxygen concentrations and that oxygenation of the fluid Earth would proceed rapidly in less than 150 kyr, a conclusion similar to the model results here. Additionally a recent study that focused on O<sub>2</sub> concentrations through Proterozoic time found that an anoxic or low-oxygen atmosphere is unstable given expectations of an oxygenic photosynthetic biosphere, and that such a system will rapidly converge to a relatively high oxygen atmosphere (Laakso and Schrag 2014). Though arrived at in a different way, the results from that study concur with our findings.

**Uncertainties** As discussed above, the most significant variable in this model concerns the fate of fixed organic carbon. As most organic carbon fixed in the modern ocean is quickly respired, the balance of O<sub>2</sub> in the atmosphere can be quickly perturbed if burial rates are altered, and uncertainty in burial efficiency introduces a large degree of uncertainty into our model results. Other factors introduce lesser uncertainty.

Another significant parameter is the proportion of carbon that is remineralized through methanogenesis. Aerobic respiration consumes O<sub>2</sub>, but if organic carbon is instead converted to methane it will be oxidized through a combination of methanotrophy—a direct or indirect sink of O<sub>2</sub>—as well as photolysis, which is largely O<sub>2</sub>-neutral in the Archean atmosphere. As a result, higher methanogenic fluxes actually contribute somewhat to the more rapid accumulation of O<sub>2</sub> in the atmosphere as they provide a sink for reducing equivalents that can be

uncoupled from O<sub>2</sub>. With a reasonable methanogenic flux of 50 % of remineralized carbon [comparable to minimum estimates for ferruginous Lake Matano (Crowe et al. 2011), and those estimated for Archean basins by Hayes (1994)], the oceans and atmosphere achieve oxygenation within ~17 kyr. A more modest methanogenic flux of 10 %, well below that of Lake Matano but comparable to that estimated for the pre-oxygenic photosynthesis Archean Earth system (Kharecha et al. 2005) results in oxygenation in about 57 kyr.

While these model calculations draw the best available constraints from theory and analog sites, the Archean Earth is largely unconstrained in many respects, so additional data could change the results. For instance, if early Cyanobacteria were more sensitive to oxygen than anticipated (e.g., by a delayed evolution of oxygen detoxification enzymes), this could in principle limit the local rates of gross primary production, though it remains unclear how significant this would be to the conclusions of our model as we assume a limitation based on nutrient availability rather than growth rate.

Although hydrothermal activity, volcanic outgassing, and crustal production rates are minor components of this model, if their rates are far higher as suggested by some authors (e.g., Kump and Barley 2007) this could delay oxygenation somewhat (though a doubling of either factor affects the time to oxygenation by no more than a few thousand years). However, because of the large difference in magnitude between primary productivity and these geological fluxes they are unlikely to impede oxygenation over geological timescales without unexplained variability through time. Moreover, it is reasonable that Archean tectonic and outgassing rates were more sluggish in the past due to thicker crust (e.g., Korenaga 2006)—even the sign of differences in these rates is uncertain.

**Reaching a new Steady State** Eventually, oxygen concentrations will stabilize and the Earth will enter a new steady state. Previous models have attempted to resolve the factors that control O<sub>2</sub> in a steady state (e.g., Lasaga and Ohmoto 2002; Laakso and Schrag 2014) but the results tend to differ between models and it is difficult to determine which if any are accurate given our current knowledge of the modern O<sub>2</sub> cycle.

The modeling approach taken here differs in that it does not explicitly evaluate how or when a new steady state will be reached, but some predictions can be made. Aerobic respiration serves as one of the most important negative feedbacks on oxygen: higher O<sub>2</sub> and increased oxygenation of the water column and shallow pore fluids promotes more efficient remineralization, limiting the accumulation of oxygen. Before respiration feedbacks take strong hold, the carbon cycle may be out of balance due to organic carbon burial rates higher than those before or since. Similar logic forms the basis for a class of interpretations of the large C isotope excursions observed in carbonate rocks ( $\delta^{13}\text{C}$  values about 10 permil higher than Archean and Palaeoproterozoic background values) associated with the rise of oxygen (Martin et al. 2013). The exact timing and duration of these isotopic excursions are not well understood (Rasmussen et al. 2013b), but they may have lasted for as much as tens to several hundred millions of years (Karhu and Holland 1996). It was suggested that oxygen may have initially accumulated to higher concentrations than supported by this steady state, leading to an initial overshoot followed by collapse before reaching the Proterozoic steady state concentration (Bekker and Holland 2012; Canfield et al. 2013). If correct, substantial amounts of inorganic carbon must be fixed and buried, possibly requiring additional inputs of carbon to the fluid Earth such as the those derived from the oxidation of siderite (Bachan and Kump 2015).

An additional impact of the rise of oxygen was the collapse of the methane greenhouse, which may have helped sustain a clement Paleoproterozoic climate. The timescales estimated for oxygenation (examples in Table 1) are in many cases sufficiently fast to have outpaced the silicate weathering feedback (e.g., Schrag et al. 2002) and triggered global glaciation—possibly marked by the low latitude glacial strata of the Makganyene Formation (Kopp et al. 2005). It is reasonable to suspect that this event included a wide range of impacts on productivity and atmospheric composition during this time.

## Conclusions

From the perspective of the calculations presented here, the characteristic timescales of environmental oxygenation [certainly the timescales required to impact sensitive redox proxies like redox-sensitive detrital grains (Johnson et al. 2014) and mass independent S isotope fractionation (Pavlov and Kasting 2002)] following the evolution of oxygenic photosynthesis are geologically rapid—unless rates of GPP are far lower than typically thought. The only way to prevent geologically rapid oxygenation of Earth surface environments once oxygenic photosynthesis has evolved is to reduce rates of primary productivity by orders of magnitude to lower than the geological fluxes of reduced compounds. It has been shown that extant Cyanobacteria experience a defect in growth rate when exposed to high dissolved iron concentrations—an effect termed anaerobic iron toxicity—suggesting that perhaps iron toxicity may have delayed oxygenation following the evolution of oxygenic photosynthesis (Swanner et al. 2015). However, the observed growth defect was relatively minor (<50 %) at the iron concentrations predicted for Archean seawater, and similar and even more severe toxicity has been shown for heterotrophs exposed to high dissolved iron concentrations (e.g., Touati 2000; Bird et al. 2013). As a result, the impact of iron toxicity on Archean net primary productivity may have been neutral or even positive. Additional physiological investigation of Cyanobacteria will be necessary to identify other potential limits to early productivity. However, no compelling argument is currently available for why Cyanobacteria would remain so unproductive over long timescales—and indeed arguments for Cyanobacterial primary production made on the relative abundance of organic carbon in shales (e.g., Lyons et al. 2014), require an explicit balance in terms of O<sub>2</sub> production and a certain degree of ecosystem dominance. Rates of photosynthesis during the rise of oxygen are also not known with any certainty, however there are good reasons to suspect that these rates were elevated above those that characterized the Archean biosphere. The aforementioned interpretations of <sup>13</sup>C-enriched isotope ratio data in many Paleoproterozoic carbonates imply a larger relative flux of sedimentary organic matter associated with the rise of oxygen (Karhu and Holland 1996; Rasmussen et al. 2013b)—this is in stark contrast to Archean carbonate platforms (Fischer et al. 2009).

A fundamental reason why oxygenic photosynthesis is viewed as such an important metabolic breakthrough is not simply because it harvests more energy than typical anaerobic metabolisms per photon, but also because the electron donor for oxygenic photosynthesis—water—is not limiting in marine environments. Anoxygenic photosynthetic microbes are commonly limited by the supply of electron donors like molecular hydrogen or ferrous iron (Kharecha et al. 2005; Fischer and Knoll 2009). The removal of this constraint would allow

Cyanobacteria to exploit a huge volume of favorable environments on the Earth surface characterized by abundant water and sunlight, with their productivity limited instead by the availability of fixed nitrogen and phosphate.

The evolution of oxygenic photosynthesis fueled a number of adaptive radiations to fill the newly opened niche space of oxygenic photosynthesis and aerobic respiration (and other new metabolic opportunities from evolving biogeochemical cycles of S and N). Adaptive radiations have long been recognized as an important force in the evolution of plant and animal clades (e.g., Gavrilets 2009), but more recently have also been observed in microbial populations (e.g., Rainey 1998). Due to their short generation times, phenotypic adaptation to novel environmental conditions and genomic evolution in bacteria occurs on short timescales even visible in laboratory experiments (Bennett et al. 1992; Barrick et al. 2009). Adaptive radiations involving increased rates of genetic diversification and adaptation commonly occur following evolutionary innovations and opening up of new niche space (Gavrilets 2005). Consequently it is reasonable to expect that Cyanobacteria rapidly adapted and became specialized within a variety of environments following the evolution of oxygenic photosynthesis. Importantly, this notion is supported by phylogenetic relationships between extant oxygenic Cyanobacteria, which show a rapid radiation following a longer branch (i.e., larger evolutionary distances) separating them from their closest nonphototrophic relatives (Shih et al. 2015). This radiation likely allowed the Cyanobacteria to quickly adapt to an oxygenic photosynthetic lifestyle and occupy new niches and environments, with a dominant role in photosynthetic ecosystems.

On the basis of the calculations here and the logic presented above, we suggest that oxygenic Cyanobacteria evolved shortly before the rise of oxygen. This finding is further consistent with recent evidence calling into doubt the syngeneity of Archean biomarkers for Cyanobacteria (French et al. 2015), evidence for a transitional manganese-oxidizing phototroph just before the rise of oxygen (Johnson et al. 2013b), as well as molecular analyses that reveal the derived position of oxygenic phototrophs within the Cyanobacteria phylum (Di Rienzi et al. 2013; Shih et al. 2013, 2015; Soo et al. 2014; Johnson et al. 2013b). This also intimates that if geochemical data interpreted as whiffs of oxygen from much earlier sedimentary successions are interpreted correctly, they might reflect sources of oxygen derived from other known abiotic [e.g., hydrogen peroxide produced photochemically (Kasting et al. 1985) or via pyrite (Borda et al. 2001) and potentially concentrated on the surface of glacial ice (Liang et al. 2006) or through atmospheric processes (Haqq-Misra et al. 2011)] and biotic [e.g., oxygen produced via catalase reactions (Blankenship and Hartman 1998) or the dismutation of nitric oxide (Ettwig et al. 2010, 2012) or chlorite (Van Ginkel et al. 1996)] sources. Alternatively, these signals could largely be the result of alteration of sedimentary strata by postdepositional fluids. While chemical imaging approaches exist for evaluating the impacts of post-depositional alteration (e.g., Johnson et al. 2013a; Fischer et al. 2014; Stefurak et al. 2015), a critical issue going forward will be constructing analytical frameworks that are able to carefully consider and avoid false positive detections of oxygenic Cyanobacteria in the early sedimentary record, particularly as geochemical techniques for O<sub>2</sub> detection continue to become more sophisticated and more sensitive.

**Acknowledgments** LMW was supported by an NSF Graduate Research Fellowship. JLK is grateful for the support of the Earth-Life Science Institute. WWF acknowledges support from the Agouron Institute, a David and Lucile Packard Foundation Fellowship for Science and Engineering, the Caltech Center for Environment-Microbe Interactions, and NSF Division of Earth Sciences award EAR-1349858. We thank Jena Johnson, Jim Hemp, Sarah Slotznick, and two anonymous reviewers for providing valuable feedback on the study.

## References

- Allwood AC, Walter M, Kamber B et al (2006) *Nature* 441:714–718
- Anbar AD, Knoll AH (2002) *Science* 297:1137–1142
- Anbar AD, Duan Y, Lyons TW et al (2007) *Science* 317:1903–1906
- Arthur MA, Dean WE, Neff ED et al (1994) *Glob Biogeochem Cycles* 8:195–217
- Bachan A, Kump LR (2015) *PNAS* 121:6562–6567
- Barrick JE, Yu DS, Yoon SH et al (2009) *Nature* 461:1243–1247
- Bekker A, Holland HD (2012) *Earth Planet Sci Lett* 317–318:295–304
- Bekker A, Holland H, Wang P et al (2004) *Nature* 427:117–120
- Bender M, Sowers T, Labeyrie L (1994) *Glob Biogeochem Cycles* 8:363–376
- Bender M, Sowers T, Lipenkov V (1999) *Deep-Sea Res* 1 46:637–654
- Bennett AF, Lenski RE, Mittler JE (1992) *Evolution* 46:16–30
- Berner RA (1982) *Am J Sci* 282:451–473
- Berner RA (1989) *Glob Planet Chang* 1:97–122
- Berner RA (2006) *Geochim Cosmochim Acta* 70:5653–5664
- Bird LJ, Coleman M, Newman D (2013) *Appl Environ Microbiol* 79:3619–3627
- Bjerrum CJ, Canfield DE (2002) *Nature* 417:159–162
- Blankenship RE, Hartman H (1998) *Trends Biochem Sci* 23:94–97
- Borda MJ, Elsetinow A, Schoonen M et al (2001) *Astrobiology* 1(3):283–288
- Bosak T, Greene S, Newman D (2007) *Geobiology* 5:119–126
- Brasier MD, Green O, Jephcoat A et al (2002) *Nature* 416:76–81
- Brock TD (1978) *Thermophilic microorganisms and life at high temperatures*. Springer, New York
- Borcks JJ, Logan G, Buick R et al (1999) *Science* 285:1033–1036
- Buick R (1992) *Science* 255:74–77
- Canfield DE (2005) *Annu Rev Earth Planet Sci* 33:1–36
- Canfield DE, Glazer A, Falkowski PG (2010) *Science* 330:192–196
- Canfield DE, Ngombi-Pemba L, Hammarlund EU et al (2013) *PNAS* 110(42):6736–16741
- Catling DC, Zahnle K, McKay C (2001) *Science* 293:839–843
- Chandler FW (1988) *Carbonates Evaporites* 3:75–94
- Cloud P (1973) *Econ Geol* 68:1135–1143
- Crowe SA, Jones CA, Katsev S et al (2008) *PNAS* 105:15938–15943
- Crowe SA, Katsev S, Leslie K et al (2011) *Geobiology* 9:61–78
- Crowe SA, Døssing LN, Beukes NJ et al (2013) *Nature* 501:535–538
- Des Marais DJ (2000) *Science* 289:1703–1705
- Di Rienzi S, Sharon I, Wrighton K et al (2013) *eLife* 2:1–25
- Ducluzeau AL, Schoepp-Cothenet B, van Lis R et al (2014) *J. R. Soc. Interface* 11
- Elderfield, H and Schultz A (1996) *Annu. Rev. Earth Planet. Sci* 24 pp191–224
- Ettwig KF, Butler M, Le Paslier D et al (2010) *Nature* 464:543–548
- Ettwig KF, Speth DR, Reimann J et al (2012) *Front Microbiol* 3:8
- Falkowski PG (2011) *Photosynth Res* 107:7–10
- Field CB, Behrenfeld M, Randerson J et al (1998) *Science* 281:237–240
- Fischer WW, Knoll AH (2009) *Bull Geol Soc Am* 121:222–235
- Fischer WW, Schroeder S, Lacassie JP et al (2009) *Precambrian Res* 169:15–27
- Fischer WW, Fike DA, Johnson JE et al (2014) *PNAS* 111:5468–5473
- French KL, Hallman C, Hope J et al (2015) *PNAS* 201419563
- Gaillard F, Scaillet B, Arndt NT (2011) *Nature* 479:229–232
- Gavrilets S, Vose A (2005) *PNAS* 102:18040–18045
- Gavrilets S, Losos JB (2009) *Science* 323:732–737
- Glasspool IJ, Scott AC (2010) *Nat Geosci* 3(9):627–630
- Goldblatt C, Lenton TM, Watson AJ (2006) *Nature* 443:683–686
- Gribaldo S, Talla E, Brochier-Armanet C (2009) *Trends Biochem Sci* 34:375–381
- Grotzinger JP, Knoll AH (1999) *Annu Rev Earth Planet Sci* 27:313–358
- Guo Q, Strauss H, Kaufman AJ et al (2009) *Geology* 37:399–402
- Haqq-Misra J, Kasting J, Lee S (2011) *Astrobiology* 11:293–302
- Hartnett H, Keil R, Hedges J et al (1998) *Nature* 391:572–575
- Hayes JM (1994) *Early life on earth*. Nobel symposium No. 84. Columbia U.P, New York, pp 220–236
- Helz GR, Bura-Nakić E, Mikac N, Ciglencečki I (2011) *Chem Geol* 284:323–332
- Hoffman PF (2013) *Chem Geol* 362:143–156
- Hofmann H, Grey K, Hickman AH, Thorpe RI (1999) *GSA Bull* 111:1256–1262

- Holland HD (1984) The chemical evolution of the atmosphere and oceans. Princeton University Press
- Holland HD (2002) *Geochim Cosmochim Acta* 66(21):3811–3826
- Hotinski RM, Kump LR, Najjar RG (2000) *Paleoceanography* 15:267–279
- Hotinski RM, Bice K, Kump L et al (2001) *Geology* 29:7–10
- Johnson JE, Webb S, Thomas K et al (2013a) *PNAS* 110:11238–11243
- Johnson JE, Webb S, Thomas K et al (2013b) *PNAS* 110:E4119–E4120
- Johnson JE, Gerpheide A, Lamb M et al (2014) *Geol Soc Am Bull* 126:813–830
- Jones CA, Crowe S, Sturm A et al (2011) *Biogeosciences* 8:2977–2991
- Karhu JA, Holland HD (1996) *Geology* 24:867–870
- Kasting JF, Holland HD, Pinto JP (1985) *J Geophys Res-Atmos* 90:10497–10510
- Kharchea P, Kasting J, Siefert J (2005) *Geobiology* 3:53–76
- Knoll AH, Golubic S (1992) In: early organic evolution pp 450–462. Springer, Heidelberg
- Kopp RE, Kirschvink J, Hilburn I et al (2005) *PNAS* 102(32):11131–11136
- Korenaga J. (2006) *Archean Geodynamics and Environments*, 7-32
- Kump, LR and Barley ME (2007) *Nature* 448pp1033-1036
- Laakso TA, Schrag DP (2014) *Earth Planet. Sci Lett* 388:81–91
- Lasaga AC, Ohmoto H (2002) *Geochim Cosmochim Acta* 66:361–381
- Lécuyer C, Ricard Y (1999) *Earth Planet Sci Lett* 165:197–211
- Liang MC, Hartman H, Kopp RE et al (2006) *PNAS* 103:18896–18899
- Lyons TW, Reinhard CT, Planavsky NJ (2014) *Nature* 506:307–315
- Martin AP, Condon DJ, Prave AR, Lepland A (2013) *Earth Sci Rev* 127:242–261
- Morford JL, Martin WR, Carney CM (2012) *Chem Geol* 324–325:73–86
- Nägler TF, Neubert N, Böttcher ME et al (2011) *Chem Geol* 289:1–11
- Owan T, Cess RD, Ramanathan V (1979) *Nature* 277:640–642
- Papineau D, Mojzsis S, Schmitt A (2007) *Earth planet. Sci Lett* 255:188–212
- Pavlov AA, Kasting JF (2002) *Astrobiology* 2(1):27–41
- Pavlov A, Kasting J, Brown LL et al (2000) *J Geophys Res* 105:11981–11990
- Pavlov AA, Kasting JF, Eigenbrode JL, Freeman KH (2001) *Geology* 29(11):1003–1006
- Paytan A, Kastner M, Chavez FP (1996) *Science* 274:1355–1357
- Planavsky NJ, Asael D, Hofmann A et al (2014) *Nat Geosci* 7:283–286
- Rainey PB, Travissano M (1998) *Nature* 394:69–72
- Rashby SE, Sessions A, Summons R et al (2007) *PNAS* 104:15099–15104
- Rasmussen B, Bekker A, Fletcher IR (2013a) *Earth planet. Sci Lett* 382:173–180
- Rasmussen B, Meier DB, Krapež B, Muhling JR (2013b) *Geology* 41:435–438
- Ricci JN, Michel A, Newman D (2015) *Geobiology* 13:267–277
- Robinson JM (1990) *Geology* 15:607–610
- Rosing MT (1999) *Science* 283:674–676
- Rosing MT, Frei R (2004) *Earth Planet Sci Lett* 217:237–244
- Sadler PM (1981) *J Geogr* 89:569–584
- Schidlowski M (1983) *Precambrian Res* 20:319–335
- Schidlowski M, Eichmann R, Junge CE (1975) *Precambrian Res* 2:1–69
- Schidlowski M, Appel PW, Eichmann R, Junge CE (1979) *Geochim Cosmochim Acta* 43:189–199
- Schopf JW (1993) *Science* 260:640–646
- Schrag DP, Berner RA, Hoffmann PF, Halverson GP (2002) *Geochemistry Geophys. Geosystems* 3, 1-21
- Severinghaus JP, Beaudette R, Headly M et al (2009) *Science* 324:1431–1434
- Shih PM (2015) *Curr Biol* 25:R192–R193
- Shih PM, Wu D, Latifi A et al (2013) *PNAS* 110:1053–1058
- Shih PM, Hemp J, Ward LM et al (2015) *PNAS*. Submitted
- Soo RM, Skennerton CT, Sekiguchi Y et al (2014) *Genome Biol Evol* 6:1031–1045
- Stefurak EJT, Fischer WW, Lowe DR (2015) *Geochim Cosmochim Acta* 150:26–52
- Stolper DA, Revsbech NP, Canfield DE (2010) *PNAS* 107(44):18755–18760
- Suwa M, Bender ML (2008) *J Geophys Res-Atmos* 113:1–9
- Swanner ED, Mloszewska v, Círpka O et al (2015) *Nat. Geosci.* 8:126–12130
- Touati D (2000) *Arch Biochem Biophys* 373:1–6
- Tyrrell T (1999) *Nature* 400(6744):525–531
- van Ginkel CG, Rikken GB, Kroon AGM, Kengen SWM (1996) *Archives of Microbiology* 166 pp321-326
- Walker JGC, Klein C, Schidlowski M et al (1983) In: *Earth's earliest biosphere: its origin and evolution* pp 260–290. Princeton University Press, Princeton
- Welander PV, Coleman ML, Sessions AL et al (2010) *PNAS* 107:8537–8542
- Williams HM, Wood BJ, Wade J et al (2012) *Earth Planet Sci Lett* 321–322:54–63